Spatiotemporal Characteristics of Meteorological Drought as a Basis for Strengthening Food Security in Banten Province

Yuli Kartiningsih[1,2]*, I Nengah Putra Apriyanto[1], Sovian Aritonang[1], Linus Yoseph Wawan Rukmono[1], Riduan[1]

[1] Republic of Indonesia Defense University, Jakarta, Indonesia

[2] Meteorology, Climatology, and Geophysics Agency (BMKG), Jakarta, Indonesia

*Corresponding author: yuly.bmkg@gmail.com

HOW TO CITE:
Yuli Kartiningsih, I Nengah Putra Apriyanto, Sovian Aritonang, Linus Yoseph Wawan Rukmono, Riduan (2026), Spatiotemporal Characteristics of Meteorological Drought as a Basis for Strengthening Food Security in Banten Province

International Journal of Special Education, 41(21s), 807-833

ABSTRACT

Meteorological drought in monsoon-dominated regions can develop across different timescales and levels of severity; consequently, monitoring based on a single precipitation-accumulation period may fail to capture the full characteristics of drought events. This study analyzes the temporal variability, frequency, duration, inter-station heterogeneity, and descriptive association of drought with the El Niño–Southern Oscillation (ENSO) in Banten Province during 1991–2024. Daily precipitation records from observation stations across Banten were aggregated into monthly totals and used to calculate the Standardized Precipitation Index (SPI) at 1-, 3-, 6-, and 12-month timescales using the Gamma distribution. The analysis was conducted for four regional groups—Greater Tangerang, Greater Serang, Pandeglang, and Lebak—using regional ensemble means and station-level statistics. The results show that SPI-1 exhibits the most rapid dry–wet fluctuations, whereas SPI-3, SPI-6, and SPI-12 identify increasingly persistent events. The highest proportion of total dry months at SPI-1 occurred in Lebak (9.80%); at SPI-3, in Greater Tangerang and Lebak (11.58% each); and at SPI-6 and SPI-12, in Pandeglang (11.91% and 11.59%, respectively). Maximum drought duration increased with SPI timescale and reached 12 months at SPI-12 in Greater Tangerang, Pandeglang, and Lebak. Station-level analysis yielded median percentages of dry months ranging from 13.36% to 16.62%, indicating that regional averages may mask localized drought events. Moderate-to-strong El Niño phases were generally associated with declining SPI values, whereas La Niña more often coincided with recovery toward normal or wet conditions, although responses varied among regions and events. These findings underscore the need for multiscale and location-specific drought monitoring. SPI-3 can support seasonal preparedness and agricultural water management, whereas SPI-12 is more relevant for assessing persistent precipitation deficits and longer-term water-resource planning.

Keywords: ENSO; food security; meteorological drought; water management; multiscale SPI.

INTRODUCTION

Drought is a hydroclimatic hazard that develops gradually yet can generate widespread and long-lasting impacts. Unlike floods, which generally have a relatively identifiable onset, drought emerges through the accumulation of precipitation deficits over weeks, months, or even years. This slow development makes the onset and termination of drought difficult to determine directly. Its impacts may propagate from reduced atmospheric water availability to declining soil moisture, reduced streamflow and surface-water storage, and ultimately disruptions to agriculture and domestic water supply. In recent decades, climate change has heightened concern over drought risk because global warming can alter precipitation patterns, increase atmospheric water demand, and intensify the interaction between rainfall deficits and water losses through evapotranspiration. Chiang et al. (2021) demonstrated an anthropogenic contribution to changes in the frequency, duration, and intensity of meteorological drought across many regions of the world. These findings are consistent with Intergovernmental Panel on Climate Change assessments indicating that very wet and very dry events are expected to intensify as global temperatures increase, although the direction and magnitude of change remain region-specific (IPCC, 2021, 2023).

Drought is not a single phenomenon but is commonly classified into meteorological, agricultural, hydrological, and socioeconomic drought. Meteorological drought occurs when precipitation falls below the climatologically expected level over a specified period. Such a deficit may represent the initial stage of agricultural drought when soil-water availability becomes insufficient to meet crop demand, and may subsequently develop into hydrological drought as river discharge, reservoir levels, and groundwater reserves decline. The transition among drought types is not necessarily direct because it is influenced by the duration of rainfall deficits, soil properties, land cover, water-resource management, cropping seasons, and local water demand. Meteorological drought therefore needs to be monitored across multiple timescales to represent system responses to short-term, seasonal, medium-term, and long-term precipitation deficits. A systematic review of Southeast Asia likewise emphasized that the choice of drought index and timescale is critical because tropical climate characteristics, monsoon systems, topography, and data availability vary substantially among regions (Zaki & Noda, 2022).

Meteorological drought variability in the tropics is governed not only by long-term climate change but also by interannual ocean–atmosphere interactions. One of the most influential phenomena is the El Niño–Southern Oscillation (ENSO), which develops from coupled changes in sea-surface temperature and atmospheric pressure over the tropical Pacific Ocean. The warm phase of ENSO, or El Niño, is generally associated with an eastward displacement of the main convective center toward the central and eastern Pacific and weakened cloud formation over parts of the Indonesian Maritime Continent. These conditions tend to suppress rainfall, particularly during the dry season and the transition toward the wet season. Conversely, the cold phase, or La Niña, usually enhances convection around Indonesia and increases the likelihood of above-normal rainfall. Nevertheless, the rainfall response to ENSO is not always linear because it depends on event intensity, timing, duration, ENSO type, and interactions with other climate systems. A strong El Niño therefore does not necessarily generate the same drought severity at every location or timescale.

Indonesia exhibits pronounced rainfall heterogeneity because it lies between the Indian and Pacific Oceans and is influenced by the Asian–Australian monsoon circulation, ENSO, the Indian Ocean Dipole (IOD), the Madden–Julian Oscillation (MJO), equatorial waves, local sea-surface temperatures, land–sea circulations, and complex topography. Ariska et al. (2024) showed that the relationships between Indo-Pacific climate modes and Indonesian rainfall vary spatially and temporally, meaning that the response observed in one region cannot be generalized directly to the entire country. Mulsandi et al. (2024) also demonstrated strong links between Indonesian monsoon rainfall, sea-surface temperature variability, and regional atmospheric circulation. In addition, the extreme positive IOD event of 2019 produced marked rainfall reductions across several parts of Indonesia, indicating that dry anomalies cannot always be explained by ENSO alone (Iskandar et al., 2022). This complexity requires ENSO-related analyses to acknowledge that local conditions and other climate phenomena can either amplify or dampen rainfall responses to Pacific sea-surface temperature anomalies.

Recent studies have demonstrated ENSO-related influences on hydrological components across Java. Nugroho et al. (2021) identified relationships between ENSO and IOD indices and variations in river-flow regimes in southern Java. Subsequent analyses of several river basins in Java showed that the strength and direction of teleconnections can vary by location, season, phase of climate development, and the streamflow characteristic being examined (Nugroho et al., 2022). These results indicate that using a single climate-index value to represent the response of the entire island may conceal important local variability. Differences in rainfall totals, seasonal regimes, geographic setting, and local water-storage capacity can produce contrasting sensitivities to El Niño and La Niña. Accordingly, analyses based on a dense observation network are required to distinguish areas that respond consistently to ENSO from those in which local factors exert a stronger influence.

Banten Province provides a relevant setting for such an assessment because rainfall regimes and water demand vary considerably among its districts and cities. In addition to sustaining population and economic activities, water availability is closely linked to the continuity of food production. Statistics of Banten Province reported that, in 2024, the province had approximately 299.09 thousand ha of harvested rice area and produced 1.55 million tonnes of dry unhusked rice, equivalent to about 883.13 thousand tonnes of rice. This production scale indicates that disruptions to water availability and shifts in the onset of the rainy season can affect planting decisions and the stability of agricultural production. At the same time, rainfall across Banten cannot be treated as spatially uniform because the northern, central, and southern parts of the province may respond differently to regional and global climate anomalies. Province-wide analysis should therefore retain information at both station and administrative-area levels so that localized dry conditions are not obscured by overly broad regional averages.

The linkage between drought and food security is best positioned as a strategic implication of climate monitoring. Precipitation deficits occurring during critical crop-growth stages can reduce soil and irrigation water availability, shift planting calendars, shorten the effective growing period, and increase the likelihood of yield losses. These effects concern not only the volume of food produced, but also production stability and the sustained ability of communities to access food. The IPCC (2023) concluded that climate change has already reduced food security and affected water security, particularly through more frequent or severe extreme events and disruptions to production systems. Saleem et al. (2025) similarly showed that climate change poses both direct and indirect threats to agricultural production and the achievement of food-security objectives. From a national-resilience perspective, information on the timing, intensity, and spatial extent of drought can support adaptation planning and risk reduction. The effectiveness of such information depends on the ability of climate services to translate data into decision-relevant knowledge, as Nocezo et al. (2024) showed that access to climate services can influence cropping decisions and household food security among smallholder farmers. The present study, however, does not measure food security directly; rather, food security is treated as an important application domain for meteorological drought information.

The Standardized Precipitation Index (SPI) is among the most widely used indicators for identifying meteorological drought. Developed by McKee et al. (1993), the SPI quantifies precipitation deficits or surpluses over a selected timescale. It is calculated by accumulating precipitation over the chosen period, fitting the accumulated values to a probability distribution, and transforming the cumulative probability to the standard normal distribution. The resulting index is dimensionless: negative values indicate drier-than-climatological conditions, whereas positive values indicate wetter conditions. This standardization enables comparison among locations with different rainfall climatologies using a common scale. The World Meteorological Organization subsequently recommended SPI as a standard index for meteorological drought monitoring because it is relatively simple, requires only precipitation data, and can be applied across diverse climatic conditions (WMO, 2012). The review by Zaki and Noda (2022) also found that SPI remains one of the most frequently applied drought indices in Southeast Asia.

A key strength of SPI is its ability to characterize drought across multiple timescales. SPI-1 reflects very short-term precipitation variability and responds rapidly to month-to-month changes. SPI-3 represents seasonal rainfall conditions relevant to crop-development stages and upper-layer soil-water availability. SPI-6 characterizes medium-term accumulated rainfall deficits, whereas SPI-12 represents more persistent annual-scale conditions that may be associated with changes in longer-term water storage. Reliance on a single timescale can therefore produce an incomplete interpretation. A dry event evident in SPI-1 may not evolve into drought at SPI-6 or SPI-12, whereas a long-term SPI can remain negative even after monthly rainfall begins to recover because it still incorporates deficits from preceding months. Research in Indonesia by Sunusi and Auliana (2025) demonstrated that SPI at different timescales can be used to identify and forecast the characteristics of dry periods. Accordingly, the joint use of SPI-1, SPI-3, SPI-6, and SPI-12 provides a more comprehensive view of drought development, persistence, and recovery.

Although drought research in Indonesia continues to expand, many studies still rely on gridded or satellite-based datasets at national or regional scales, whereas others focus on a single river basin or a single SPI timescale. Gridded and remotely sensed products are valuable for providing spatially consistent coverage, particularly where observation networks are sparse. However, such products may smooth local rainfall variability, especially in areas with strong rainfall gradients or uneven station distribution. Reviews of Earth-observation applications for drought in Southeast Asia also document the growing use of satellite products and vegetation indices while emphasizing that data selection and validation must be tailored to the characteristics of the study region. Meanwhile, teleconnection studies in Indonesia have shown that rainfall and streamflow responses to ENSO are spatially heterogeneous. On the basis of the literature reviewed here, studies integrating long-term station rainfall records, multiscale SPI, and ENSO analysis for the entirety of Banten Province remain limited. This statement refers to the scope of the literature examined and does not imply that no drought studies have ever been conducted at individual locations in Banten.

A further limitation concerns how ENSO responses are represented. Province-wide mean rainfall or a single regional SPI series may conceal important inter-location differences. For example, a regional median indicating normal conditions may coexist with severe drought at several stations. In addition, the ENSO signal may appear strong at short SPI timescales but weaker at longer timescales, or vice versa, depending on the onset, peak, and termination of an ENSO event. Analyses that distinguish only between El Niño and non-El Niño years without considering event intensity and drought timescale can therefore oversimplify a complex relationship. An appropriate approach should retain inter-station variability while also producing regionally interpretable information for decision-making. It should likewise avoid assuming that every drought event is caused by ENSO, given that Indonesian rainfall is also shaped by the IOD, monsoon variability, intraseasonal processes, local sea-surface temperatures, and other atmospheric mechanisms.

This study addresses these gaps by analyzing meteorological drought in Banten Province using daily precipitation records from 85 stations for 1991–2024. Daily observations were aggregated into monthly rainfall totals and used to calculate SPI at 1-, 3-, 6-, and 12-month timescales. Inter-station information was then evaluated temporally and spatially and summarized by district/city and regional group, thereby preserving local variability while generating information relevant at administrative scales. ENSO variability was represented by the Niño3.4 index to evaluate how ENSO phase and intensity are associated with drought conditions across different timescales. The novelty of the study lies in integrating a relatively dense station network, an observation period exceeding three decades, multiscale SPI analysis, and an assessment of drought responses to ENSO at both station and administrative-region levels in Banten. This framework is designed to reveal whether drought responses to ENSO are spatially uniform or instead exhibit location-specific sensitivities and timescale dependence.

Against this background, the study aims to: (1) identify the temporal and spatial characteristics of meteorological drought in Banten Province using SPI-1, SPI-3, SPI-6, and SPI-12; (2) evaluate the association between ENSO phase and intensity and meteorological drought occurrence across multiple timescales; and (3) identify areas exhibiting the most consistent or strongest drought responses to ENSO. The results are expected to strengthen understanding of ENSO–drought teleconnections in western Java and provide a scientific basis for more location-specific drought monitoring and early-warning systems. More broadly, the resulting information can support water-resource management, adjustment of planting calendars, and reduction of risks to the stability of food production as an important component of regional resilience.

2. METHODOLOGY

This study applies temporal and spatiotemporal analyses to identify the characteristics of multiscale meteorological drought and its temporal association with El Niño–Southern Oscillation (ENSO) variability in Banten Province from January 1991 to December 2024. The primary dataset consists of daily precipitation observations obtained from the Meteorology, Climatology, and Geophysics Agency (BMKG) through the observation database of the Banten Class I

Climatology Station. The initial database contained 87 stations or rain-gauge posts. Following quality control and checks of data completeness and regional metadata, 85 stations were retained for regional analysis: 23 in Greater Tangerang, 18 in Greater Serang, 13 in Pandeglang, and 31 in Lebak.

Tangerang Regency, Tangerang City, and South Tangerang City were grouped as Greater Tangerang, whereas Serang Regency, Serang City, and Cilegon City were grouped as Greater Serang. Pandeglang Regency and Lebak Regency were analyzed as separate regions. This grouping was used to generate regional information without discarding station-level results. Administrative boundaries were obtained from the Ina-Geoportal of the Geospatial Information Agency, while station locations were determined from latitude and longitude coordinates in the observation metadata. The resulting regional grouping is shown in Figure 1.

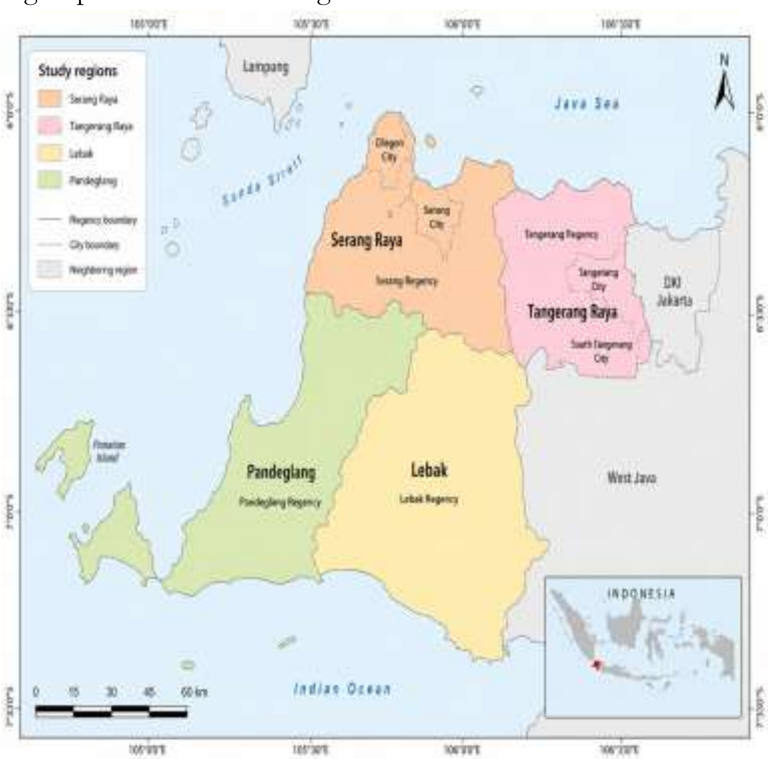

Figure 1. Location of the study area in Banten Province.

Precipitation data were checked for date and unit consistency, negative values, duplicate records, missing data, and inconsistencies in station identity. Invalid observations were excluded, while daily data that passed quality control were aggregated into monthly precipitation totals for each station. Months that did not satisfy the completeness criteria were excluded from probability-distribution fitting. Monthly precipitation totals were subsequently accumulated using moving windows of 1, 3, 6, and 12 months:

$$X_{i,t}^{(k)} = \sum_{j=0}^{k-1} P_{i,t-j}, \quad k \in \{1,3,6,12\} \tag{1}$$

where $X_{i,t}^{k}$ denotes accumulated precipitation at station i, time t, and timescale k months, while $P_{i,t-j}$ is the monthly precipitation total at month t−j. SPI-1 was used to characterize short-term precipitation deficits or surpluses; SPI-3 represents seasonal conditions; SPI-6 captures medium-term accumulated rainfall deficits; and SPI-12 represents more persistent annual-scale conditions. Multiple timescales are required because drought development can differ substantially between monthly, seasonal, and annual periods (McKee et al., 1993; WMO, 2012; Zaki & Noda, 2022; Sunusi & Auliana, 2025).

The Standardized Precipitation Index was calculated separately for each station, calendar month, and timescale. Thus, accumulated precipitation ending in a given month was compared only with historical values ending in the same calendar month. This approach prevents the standardization process from being distorted by climatological differences between the wet and dry seasons. Accumulated precipitation was fitted to a Gamma distribution, whose probability-density function is expressed as:

$$g(x;\alpha,\beta) = \frac{x^{\alpha-1}e^{-x/\beta}}{\beta^{\alpha}\Gamma(\alpha)}, \quad x > 0 \tag{2}$$

where x denotes accumulated precipitation, α is the shape parameter, β is the scale parameter, and Γ(α) is the Gamma function. Distribution parameters were estimated separately for each station, calendar month, and SPI timescale using maximum likelihood estimation. This procedure ensures that rainfall characteristics at one station are not assumed to be identical to those at another, and that wet-season distributions are not conflated with dry-season distributions. The Gamma distribution is among the most widely used parametric approaches for SPI calculation, although its goodness of fit should still be evaluated, particularly in the distribution tails (McKee et al., 1993; Guttman, 1999; WMO, 2012; Vangelis & Kourtis, 2025).

Because the Gamma distribution is defined only for values greater than zero, whereas monthly precipitation series may contain zero values, the probability of zero precipitation must be incorporated into the cumulative probability. If m is the number of zero-precipitation observations and n is the total number of valid observations, the probability of zero precipitation is q = m/n. The cumulative probability after accounting for zero rainfall is calculated as follows:

$$H(x) = q + (1-q)G(x) \tag{3}$$

where G(x) is the cumulative probability of the Gamma distribution and H(x) is the cumulative probability corrected for zero-precipitation occurrence. This probability is then transformed to the standard normal distribution to obtain SPI using the following equation:

$$SPI_{i,t}^{(k)} = \Phi^{-1}\left[H\left(X_{i,t}^{(k)}\right)\right] \tag{4}$$

where Φ^{-1} denotes the inverse standard normal cumulative distribution function. The period 1991–2024 was used as the reference period, so the SPI value represents the relative position of precipitation within the historical distribution for the same station, calendar month, and timescale (Guttman, 1999; WMO, 2012).

SPI values were classified as extremely dry (SPI ≤ −2.00), severely dry (−2.00 < SPI ≤ −1.50), moderately dry (−1.50 < SPI ≤ −1.00), near normal (−1.00 < SPI < 1.00), moderately wet (1.00 ≤ SPI < 1.50), severely wet (1.50 ≤ SPI < 2.00), and extremely wet (SPI ≥ 2.00). Meteorological drought was identified when SPI reached −1.00 or lower, consistent with McKee et al. (1993) and WMO (2012).

Regional conditions were calculated using the ensemble mean of all stations with valid data for each region, month, and SPI timescale:

$$\overline{SPI}_{r,t}^{(k)} = \frac{1}{n_{r,t}}\sum_{i=1}^{n_{r,t}} SPI_{i,t}^{(k)}$$

where $SPI_{r,t}^{k}$ is the ensemble mean for region r, time t, and timescale k, and $n_{r,t}$ is the number of stations with valid data. The 25th and 75th percentiles were calculated to characterize inter-station variability. Temporal plots display the series for individual stations, the regional ensemble mean, and the P25–P75 band so that localized drought can remain visible even when the regional condition is classified as normal. A multiscale, multi-station approach is important because drought characteristics can vary among locations and according to the selected timescale (Dabanlı et al., 2017; Zaki & Noda, 2022; Worku, 2024).

Drought frequency was calculated as the percentage of months with SPI ≤ −1.00 relative to all valid months:

$$F_r^{(k)} = \frac{N_{r,\,SPI \leq -1}^{(k)}}{N_{r,\,valid}^{(k)}} \times 100\%$$

Drought frequency was further separated into moderately dry, severely dry, and extremely dry categories. Drought duration was defined as the number of consecutive months for which the regional ensemble mean had SPI ≤ −1.00, and maximum duration was the longest drought sequence for each region and SPI timescale. Inter-station heterogeneity was analyzed using the percentage of dry months at each station and summarized by the median, 25th and 75th percentiles, and minimum–maximum range. The analysis also identified the stations with the highest drought frequency and the stations recording the minimum SPI values. These distributions were visualized using boxplots with station points, while spatiotemporal patterns were represented using SPI-3 and SPI-12 matrices. This approach enables the simultaneous evaluation of differences in drought frequency, intensity, and persistence among locations (Dabanlı et al., 2017; Guo et al., 2017; Worku, 2024).

ENSO variability was represented using monthly Niño3.4 sea-surface temperature anomalies for 1991–2024 from the NOAA Extended Reconstructed Sea Surface Temperature version 5 (ERSSTv5) product. Niño3.4 is the average sea-surface temperature anomaly over 5°N–5°S and 170°W–120°W in the tropical Pacific Ocean. ERSSTv5 provides a long-term reconstruction of sea-surface temperature that is widely used for ENSO monitoring and analysis (Huang et al., 2017; NOAA Physical Sciences Laboratory, n.d.).

For comparison with SPI-3, a three-month running mean of Niño3.4 was used. Moderate El Niño was identified when the anomaly reached ≥1.0°C and strong El Niño when it reached ≥1.5°C; moderate La Niña was identified when the anomaly was ≤−1.0°C and strong La Niña when it was ≤−1.5°C. For SPI-12, the annual ENSO category was defined operationally from the monthly Niño3.4 anomaly with the largest absolute magnitude within the same year. If both positive and negative anomalies meeting the threshold occurred in one year, the category with the larger absolute magnitude was selected as the dominant condition. These categories were used as operational visual markers and were not intended to represent the official ENSO classification based on the Oceanic Niño Index. The use of Niño3.4 and a three-month accumulation period is consistent with ENSO as an ocean–atmosphere mode that develops over several months, while rainfall responses may still vary by event intensity, season, and regional characteristics (Santoso et al., 2017; McPhaden et al., 2020).

Moderate-to-strong El Niño and La Niña periods were shown as vertical shading on the SPI-3 and SPI-12 plots. This pairing was used to examine temporal correspondence between changes in Niño3.4 and the development of dry or wet conditions. The ENSO analysis is descriptive; it was not used to estimate statistical association strength or infer causality with SPI. Such caution is necessary because Indonesian rainfall is also influenced by the IOD, monsoon variability, MJO, local sea-surface temperatures, and other atmospheric processes (Hendon, 2003; As-syakur et al., 2014; Iskandar et al., 2022; Ariska et al., 2024).

All data processing, SPI calculations, statistical analyses, and visualizations were performed in Python. Results are presented as multiscale temporal plots, frequency and duration tables, severity diagrams, inter-station boxplots, SPI-3 and SPI-12 spatiotemporal matrices, and plots comparing SPI with ENSO variability. The overall research workflow is shown in Figure 2.

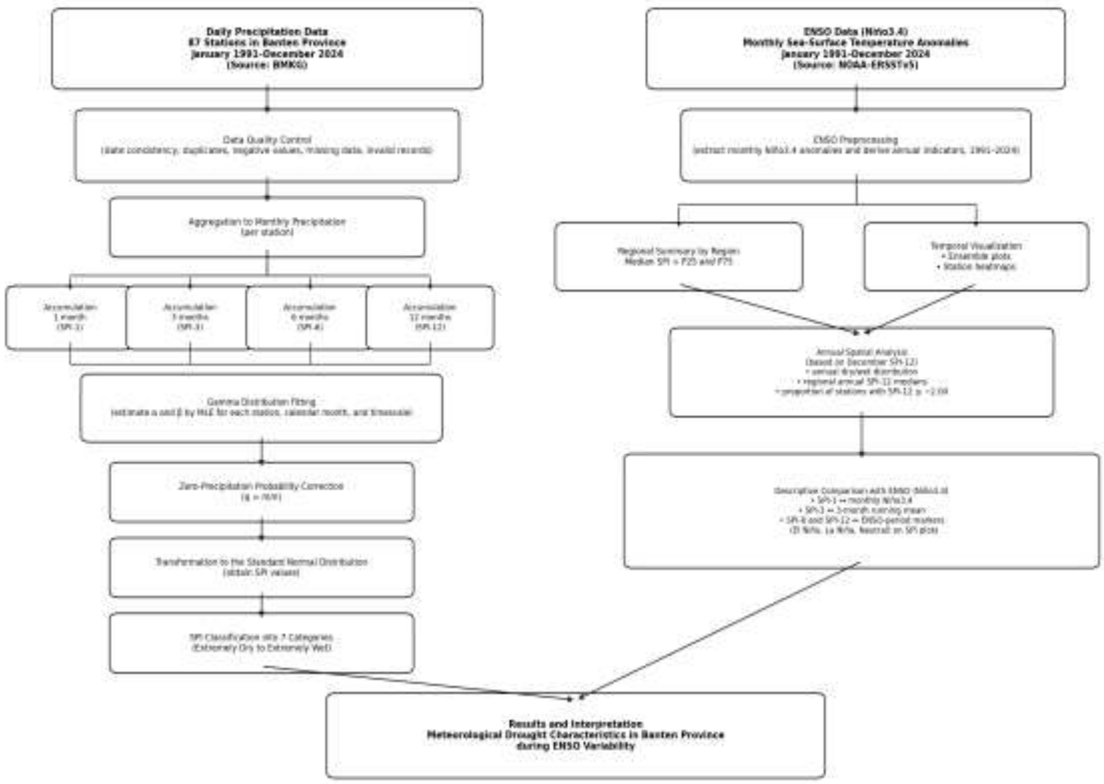

Figure 2. Research workflow.

. RESULTS AND DISCUSSION

3.1 Temporal variability of multiscale meteorological drought

Figures 3 and 4 show that dry and wet conditions in Banten fluctuated throughout 1991–2024, with patterns varying systematically by timescale. SPI-1 exhibited the sharpest changes and the most rapid transitions because of its sensitivity to monthly precipitation anomalies. Variability became progressively smoother at SPI-3 and SPI-6, whereas SPI-12 identified more persistent episodes of precipitation deficit or surplus. This pattern is consistent with Zhu et al. (2024), who reported that SPI sensitivity decreases and its fluctuations become more stable as the precipitation-accumulation period increases.

The spread of individual-station series around the ensemble mean indicates that drought does not always occur uniformly within a region. During several periods, the regional mean remained within normal or moderately dry conditions while the minimum value at an individual station had already reached the severely or extremely dry category. These local extremes are visible in the lower shaded areas below thresholds of −1.5 and −2.0. The result demonstrates that reliance on a regional value alone can mask extreme local events. This finding is consistent with Worku (2024), who identified differences in drought frequency and magnitude among stations and emphasized the importance of accounting for local variability in drought analysis.

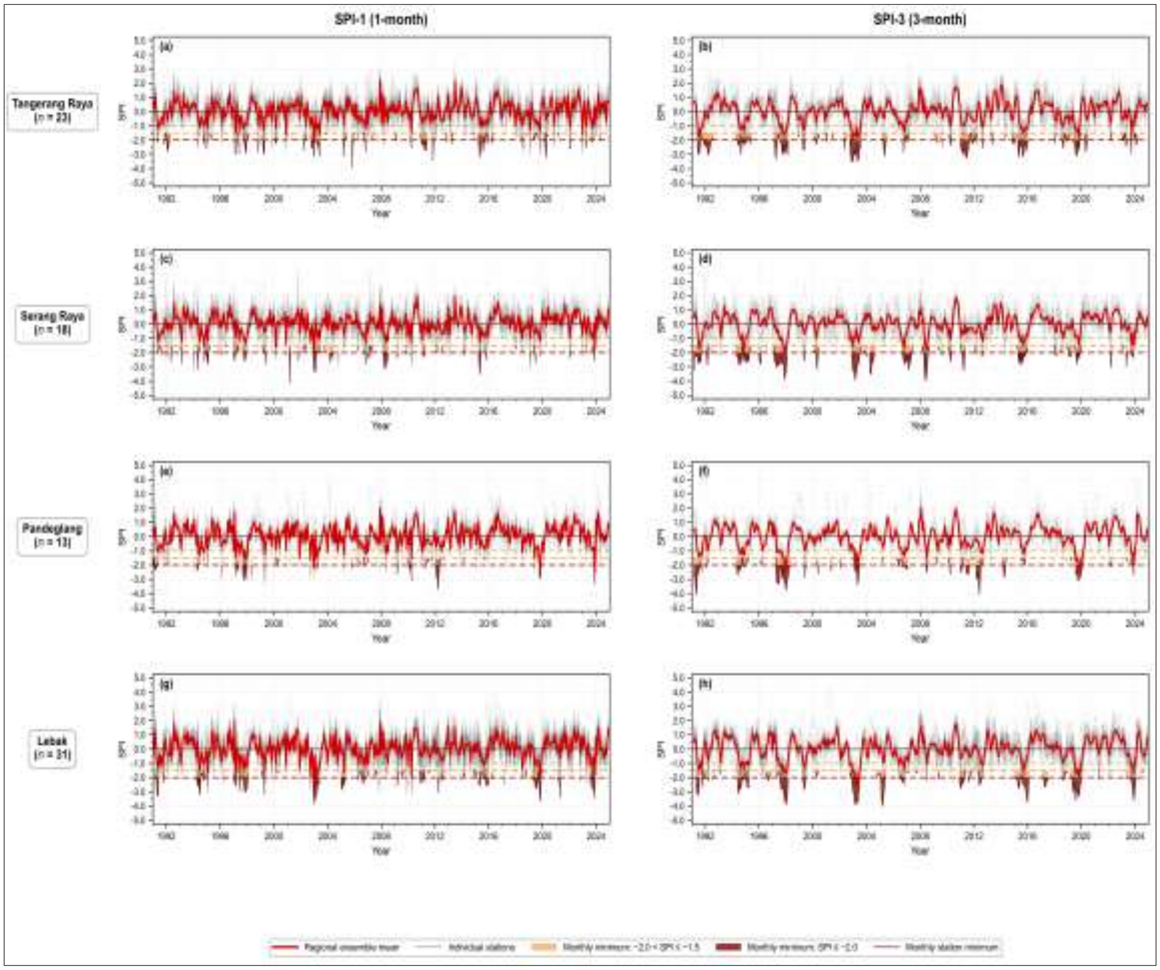

Figure 3. Temporal variability of SPI-1 and SPI-3 in Greater Tangerang, Greater Serang, Pandeglang, and Lebak during 1991–2024.

Although SPI patterns become smoother at longer timescales, this does not necessarily imply weaker drought. Accumulated rainfall deficits over several months can produce longer and more severe events. Chakma et al. (2025), for example, found greater drought duration and severity at SPI-3 than at SPI-1. The present results therefore confirm that SPI-1 is better suited to detecting short-term changes, whereas SPI-3, SPI-6, and SPI-12 are more effective for identifying the development and persistence of seasonal-to-annual drought.

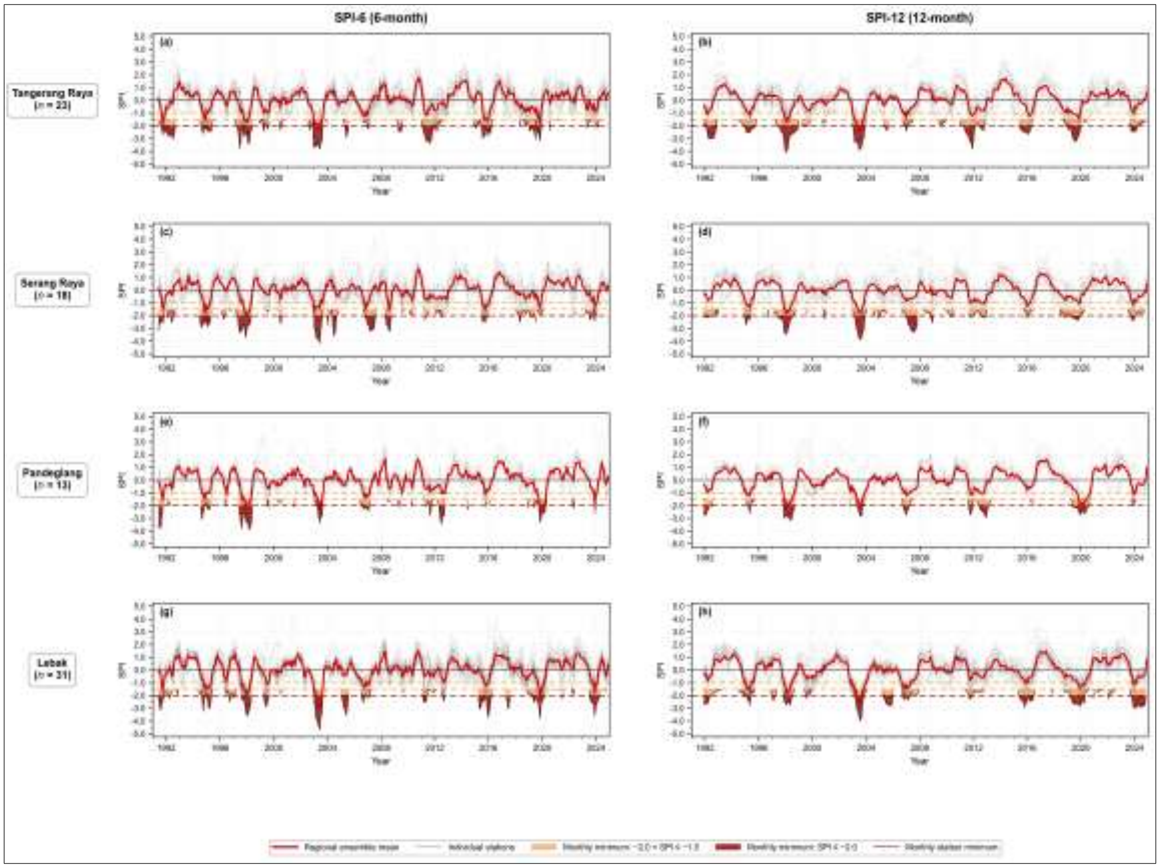

Figure 4. Temporal variability of SPI-6 and SPI-12 in Greater Tangerang, Greater Serang, Pandeglang, and Lebak during 1991–2024.

3.2 Drought frequency and severity

The frequency, severity, and duration of meteorological drought were analyzed from regional ensemble-mean values at SPI-1, SPI-3, SPI-6, and SPI-12. Drought events were classified as moderately dry ($-1.5 < \text{SPI} \leq -1.0$), severely dry ($-2.0 < \text{SPI} \leq -1.5$), and extremely dry ($\text{SPI} \leq -2.0$). The number of valid months decreased from 408 at SPI-1 to 397 at SPI-12 because longer accumulation windows leave several early months in the time series without valid SPI values.

As shown in Table 1, the total frequency of dry months varied substantially by region and timescale. At SPI-1, Lebak had the highest proportion of dry months (9.80%), followed by Pandeglang (8.09%), Greater Tangerang (6.86%), and Greater Serang (5.39%). This pattern indicates that short-term precipitation deficits occurred more frequently in Lebak than in the other three regions. Lebak's SPI-1 drought frequency was dominated by moderately dry conditions (7.35%), while severely dry and extremely dry conditions accounted for only 1.96% and 0.49%, respectively. A similarly rapid response of SPI-1 to monthly rainfall variability was reported for Kotabumi, Lampung, where SPI-1 displayed high temporal variability and captured short but intense rainfall-deficit events (Ismail et al., 2025).

Table 1. Frequency, severity, and duration of meteorological drought based on regional ensemble means for SPI-1, SPI-3, SPI-6, and SPI-12 during 1991–2024.

Region	SPI scale	Valid months	Moderate dry (%)	Severe dry (%)	Extreme dry (%)	Total dry months (%)	Minimum SPI date	Max. duration (months)
Greater Tangerang	SPI-1	408	5.88	0.74	0.25	6.86	1/1/2003	2
Greater Tangerang	SPI-3	406	9.11	2.46	0.00	11.58	1/1/2003	10
Greater Tangerang	SPI-6	403	5.46	3.72	0.50	9.68	6/1/2003	9
Greater Tangerang	SPI-12	397	7.30	1.51	1.01	9.82	8/1/2003	12
Greater Serang	SPI-1	408	4.41	0.74	0.25	5.39	1/1/2003	2
Greater Serang	SPI-3	406	5.91	1.97	0.25	8.13	12/1/1997	5
Greater Serang	SPI-6	403	6.70	2.73	0.00	9.43	12/1/1997	7
Greater Serang	SPI-12	397	5.79	1.76	0.00	7.56	2/1/1998	8
Pandeglang	SPI-1	408	6.37	0.98	0.74	8.09	12/1/2023	3
Pandeglang	SPI-3	406	7.64	1.72	1.23	10.59	11/1/2019	8
Pandeglang	SPI-6	403	7.20	3.23	1.49	11.91	11/1/2019	10
Pandeglang	SPI-12	397	7.05	4.28	0.25	11.59	2/1/1998	12
Lebak	SPI-1	408	7.35	1.96	0.49	9.80	1/1/2003	4
Lebak	SPI-3	406	8.13	2.71	0.74	11.58	5/1/2003	10
Lebak	SPI-6	403	7.44	2.23	1.74	11.41	6/1/2003	9
Lebak	SPI-12	397	7.81	1.76	1.26	10.83	8/1/2003	12

The drought pattern changed when the accumulation period was extended to three months. At SPI-3, the highest proportion of dry months was identical in Greater Tangerang and Lebak (11.58% each), followed by Pandeglang (10.59%) and Greater Serang (8.13%). The increase from SPI-1 to SPI-3 occurred in all regions but was greatest in Greater Tangerang, where the proportion rose from 6.86% to 11.58%. This indicates that some rainfall deficits in Greater Tangerang were not especially pronounced at the monthly scale but became clearer after rainfall was accumulated over three months. This result agrees with findings from Lampung showing that SPI-3 provides a more stable representation of rainfall deficits by reducing month-to-month variability and capturing accumulated seasonal rainfall shortages (Ismail et al., 2025).

At SPI-6, Pandeglang recorded the highest proportion of dry months (11.91%), followed by Lebak (11.41%), Greater Tangerang (9.68%), and Greater Serang (9.43%). Pandeglang also showed contributions of 3.23% from severely dry and 1.49% from extremely dry conditions. The highest proportion of extremely dry months at this timescale occurred in Lebak (1.74%). These results indicate that, at the seasonal-to-medium-term scale, Pandeglang and Lebak not only experienced relatively high drought frequencies but also larger contributions from severe and extreme events than Greater Tangerang and Greater Serang. Such regional differences confirm that drought does not develop uniformly across space. Research in Sumatra likewise identified distinct spatial patterns of extreme drought, with some areas more frequently exhibiting extreme conditions, particularly at SPI-12, supporting the need to retain region-specific analysis even when the same drought index is applied (Suhadi et al., 2023).

At SPI-12, Pandeglang continued to record the highest proportion of dry months (11.59%), followed by Lebak (10.83%), Greater Tangerang (9.82%), and Greater Serang (7.56%). Although the percentage of extremely dry months in Pandeglang decreased to 0.25%, the region had the highest proportion of severely dry months (4.28%). In contrast, the contribution of extremely dry conditions was greater in Lebak and Greater Tangerang, at 1.26% and 1.01%, respectively. Greater Serang recorded no extremely dry events at either SPI-6 or SPI-12. Overall, Greater Serang exhibited lower drought frequency and severity, whereas Pandeglang and Lebak were more prominent at seasonal-to-annual accumulation scales.

Figure 5 shows that moderately dry conditions dominated total drought occurrence across all regions and SPI timescales. The contribution of this category ranged from 4.41–7.35% at SPI-1, 5.91–9.11% at SPI-3, 5.46–7.44% at SPI-6, and 5.79–7.81% at SPI-12. Although severely and extremely dry categories represented smaller proportions, they are important because they indicate stronger precipitation-deficit episodes. The dominance of moderately dry conditions also demonstrates that a high total proportion of dry months does not necessarily result from numerous extreme events; it may instead arise from more frequent moderate drought.

Maximum drought duration increased as the SPI accumulation period lengthened. At SPI-1, the maximum duration ranged from two months in Greater Tangerang and Greater Serang to four months in Lebak. At SPI-3, it increased to five months in Greater Serang, eight months in Pandeglang, and ten months in both Greater Tangerang and Lebak. At SPI-6, the longest episodes lasted seven months in Greater Serang, nine months in Greater Tangerang and Lebak, and ten months in Pandeglang. At SPI-12, maximum duration reached 12 months in Greater Tangerang, Pandeglang, and Lebak, compared with eight months in Greater Serang. This increase is consistent with the multiscale nature of SPI: shorter accumulation periods fluctuate more rapidly, whereas longer periods produce smoother signals that can persist for longer. A comparable pattern was reported in Mauritius, where drought episodes at SPI-12 and SPI-24 lasted longer than those at shorter timescales (Mungul & Nowbuth, 2025).

The present results, however, are not fully consistent with findings from Merauke, where short-term drought at one- to three-month timescales occurred more frequently and drought persisting beyond six months was comparatively rare (Rum et al., 2025). In Banten, the total proportion of dry months at SPI-3, SPI-6, or SPI-12 was generally higher than at SPI-1. This contrast indicates that the relationship between SPI timescale and drought frequency is not universal but depends on local rainfall characteristics, seasonality, the period of record, and geographic setting.

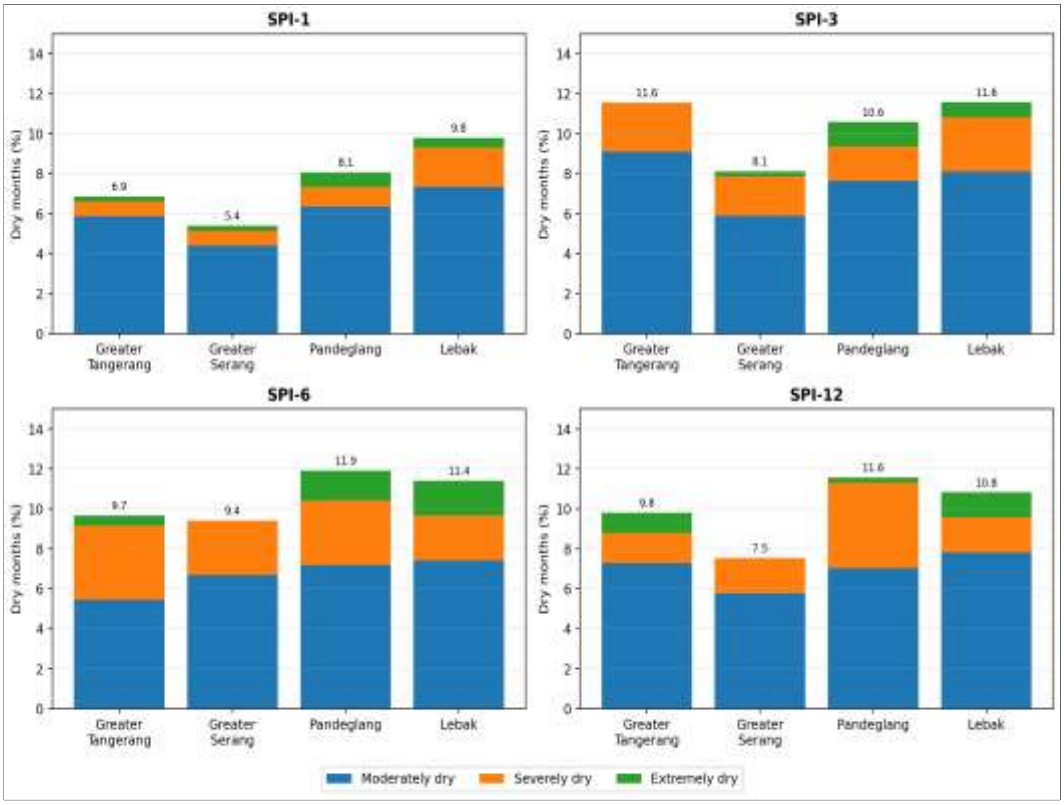

Figure 5. Percentage of meteorological drought occurrence by region, SPI timescale, and severity during 1991–2024.

Cross-timescale comparisons should also be interpreted cautiously. SPI is based solely on precipitation and therefore represents precipitation deficit rather than the full atmospheric demand affecting water availability. A comparison of SPI and SPEI in Mauritius showed that SPEI can be more responsive to dry conditions because it incorporates temperature and evapotranspiration, although the two indices remain strongly related. The present findings are therefore appropriate for describing precipitation-based meteorological drought but do not directly represent drought intensified by rising temperatures or increased atmospheric evaporative demand (Mungul & Nowbuth, 2025).

3.3 Inter-station drought heterogeneity

Station-level analysis showed that drought frequency was not uniformly distributed within each regional group. Heterogeneity was evaluated from the percentage of months with SPI ≤ -1.0 at each station. Table 2 summarizes the median, interquartile range, minimum–maximum range, the station with the highest percentage of dry months, and the minimum SPI value for each region and timescale. Figure 6 illustrates the distribution shape and the position of individual stations relative to the regional median

.Table 2. Inter-station variability in drought frequency by region and SPI timescale during 1991–2024.

Region	SPI scale	No. of stations	Median dry months (%)	Q1–Q3 (%)	Min–max (%)	Highest station (%)	Minimum SPI among stations
Greater Tangerang	SPI-1	23	15.69	11.89–16.67	9.07–18.14	Staklim Banten (18.14)	−3.88; UPTD Balaraja; Nov 2005
	SPI-3	23	16.50	15.39–17.12	12.81–19.70	UPTD Cipondoh (19.70)	−3.56; Stamet Soetta; Dec 2002
	SPI-6	23	16.38	15.88–16.75	12.41–19.11	UPTD Cipondoh (19.11)	−3.84; BPP Kaliasin; Jun 2003
	SPI-12	23	16.62	14.61–17.63	10.59–18.64	UPTD Bendung Ciputat (18.64)	−4.12; UPTD Teluk Naga; Jan 1998
Greater Serang	SPI-1	18	13.36	11.52–14.95	9.58–16.91	Stamar Serang (16.91)	−4.11; Petir; Mar 2001
	SPI-3	18	15.76	15.02–16.63	13.30–17.00	Pedarincang (17.00)	−4.00; Kasemen Kilasah; Jun 2008
	SPI-6	18	15.76	15.38–16.56	13.65–18.86	Ragas Hilir (18.86)	−4.17; Stamar Serang; Jun 2003
	SPI-12	18	16.24	15.24–17.63	14.11–21.66	Ragas Hilir (21.66)	−3.90; Stamar Serang; Aug 2003
Pandeglang	SPI-1	13	13.48	12.99–14.22	11.03–18.38	Pulosari (18.38)	−3.70; Cikeusik; Apr 2012
	SPI-3	13	16.01	15.52–16.26	12.81–17.73	Pulosari (17.73)	−4.07; Jiput; May 1991
	SPI-6	13	15.38	14.64–15.88	14.39–17.87	Cimanggu (17.87)	−3.84; Jiput; Aug 1991
	SPI-12	13	15.62	14.36–16.62	13.35–17.88	Munjul (17.88)	−3.20; Cibaliung; Jun 1998
Lebak	SPI-1	31	15.20	14.16–16.18	11.52–17.89	Cijaku (17.89)	−3.81; Cicinta; Jan 2003
	SPI-3	31	15.76	15.27–16.56	12.81–18.47	Bojong Manik (18.47)	−4.04; Warung Gunung; Mar 2005
	SPI-6	31	15.62	14.64–16.25	12.66–18.11	Banjarsari (18.11)	−4.70; Cicinta; Jun 2003
	SPI-12	31	16.45	14.61–17.35	13.10–22.42	Banjar Irigasi (22.42)	−3.98; Cisalak Baru; Aug 2003

The distributions in Figure 6 further illustrate the inter-station variability summarized in Table 2. At SPI-1, the highest median percentage of dry months occurred in Greater Tangerang (15.69%), followed by Lebak (15.20%), Pandeglang (13.48%), and Greater Serang (13.36%). Inter-station variability was greatest in Greater Tangerang, with an interquartile range of 11.89–16.67% and a full range of 9.07–18.14%. Greater Serang also showed a relatively broad range of 9.58–16.91%. By contrast, the station distribution in Pandeglang was more concentrated, with an interquartile range of only 12.99–14.22%, although one station, Pulosari, reached 18.38% dry months.

The relatively broad spread at SPI-1 indicates that short-term rainfall deficits can occur locally and are not necessarily experienced simultaneously by all stations within a region. This is reflected in the wider scatter of station points, particularly in Greater Tangerang and Greater Serang. The finding is consistent with Dabanlı et al. (2017), who analyzed 250 rain gauges and identified substantial spatial variability in SPI drought characteristics, with patterns of heterogeneity differing by timescale

.

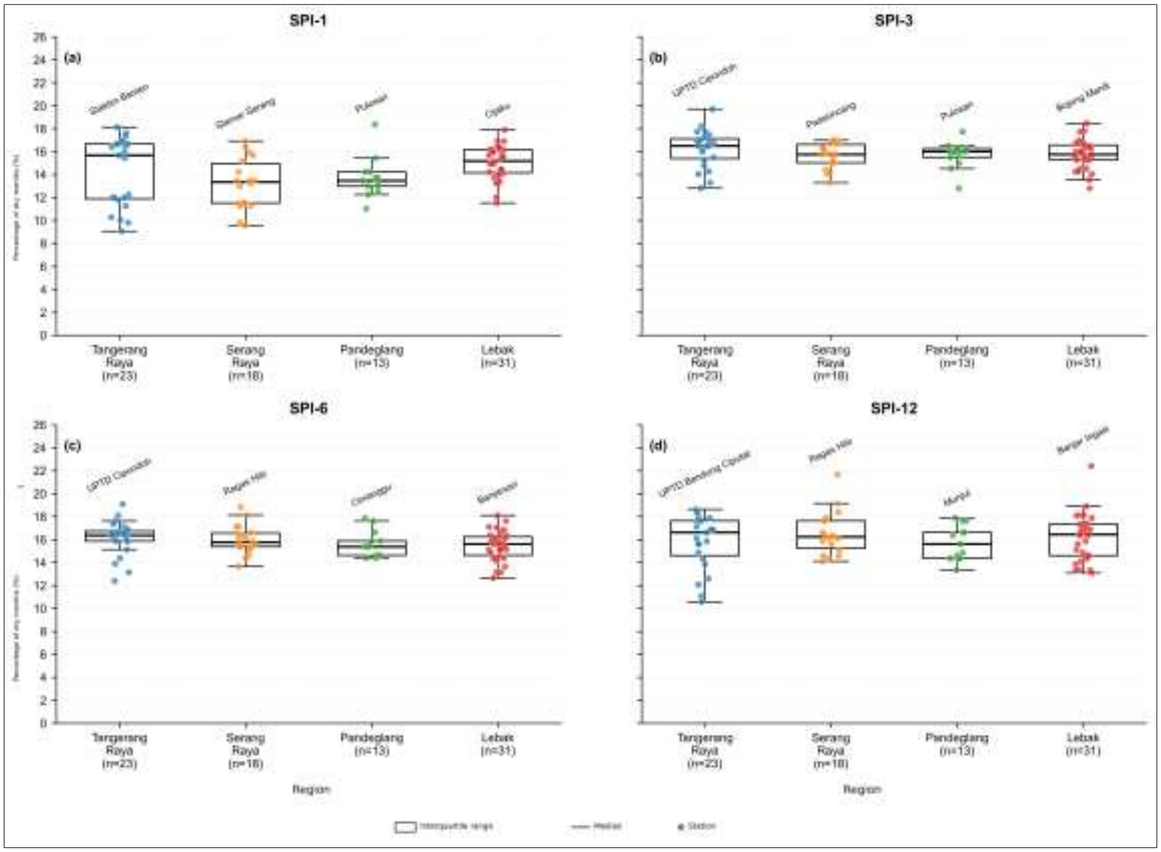

Figure 6. Distribution of the percentage of dry months among stations by region and SPI timescale during 1991–2024.

At SPI-3, the distribution of dry-month percentages became more concentrated than at SPI-1. Regional medians fell within a relatively narrow range of 15.76–16.50%. Greater Tangerang had the highest median (16.50%), while Greater Serang and Lebak shared the same median (15.76%). Interquartile ranges also narrowed, particularly in Pandeglang, where the range was only 15.52–16.26%. These results suggest that when rainfall is accumulated over three months, differences in drought frequency among stations become smaller and drought patterns become more spatially coherent at the regional scale.

Nevertheless, several stations continued to exhibit higher values than others. UPTD Cipondoh recorded the highest proportion of dry months in Greater Tangerang (19.70%), whereas Bojong Manik was highest in Lebak (18.47%). These differences indicate that three-month accumulation reduces short-term variability but does not eliminate local heterogeneity. A station-based event-frequency approach was also applied by Ipek et al. (2025) across 224 stations, showing that station-level probabilities of drought categories can reveal spatial boundaries and variability that are not apparent from a single regional value.

At SPI-6, the median percentage of dry months ranged from 15.38% in Pandeglang to 16.38% in Greater Tangerang. Interquartile ranges were relatively narrow in all regions, particularly in Greater Tangerang (15.88–16.75%) and Greater Serang (15.38–16.56%). This pattern indicates that seasonal-to-medium-term drought frequency was more uniform among stations than monthly drought frequency. Despite the more concentrated distributions, stations with relatively high values remained evident, including UPTD Cipondoh in Greater Tangerang (19.11%), Ragas Hilir in Greater Serang (18.86%), Cimanggu in Pandeglang (17.87%), and Banjarsari in Lebak (18.11%).

The distinction between drought frequency and intensity is also evident from the fact that the station with the highest percentage of dry months was not always the station with the lowest minimum SPI. For example, at SPI-6 in Lebak, Banjarsari had the highest drought frequency, whereas the lowest SPI was recorded at Cicinta (−4.70) in June 2003. A similar pattern occurred in Greater Serang, where Ragas Hilir had the highest frequency but the most negative SPI was observed at Stamar Serang (−4.17). Thus, a station that experiences drought more frequently does not necessarily experience the most extreme drought intensity. Frequency and intensity should therefore be treated as distinct drought characteristics.

At SPI-12, inter-station variability widened again in several regions. Greater Serang exhibited a full range of 14.11–21.66%, while Lebak reached 13.10–22.42%. The maxima in these two regions occurred at Ragas Hilir and Banjar Irigasi, respectively, and both points lay well above most of the corresponding station distributions in Figure 6. Greater Tangerang also displayed a broad range of 10.58–18.64%, with UPTD Bendung Ciputat recording the highest proportion. By contrast, Pandeglang had a narrower range of 13.35–17.88%, indicating relatively greater uniformity in annual-scale drought frequency among its stations.

The widening distributions at SPI-12 show that long-term accumulation does not necessarily increase spatial homogeneity. In some regions, 12-month accumulated rainfall deficits accentuated differences between stations that consistently experienced rainfall shortages and stations that were less frequently dry. The influence of timescale on inter-station heterogeneity is therefore nonlinear. Distributions were comparatively broad at SPI-1, narrowed at SPI-3 and SPI-6, and widened again at SPI-12, particularly in Greater Serang and Lebak. This behavior supports multiscale studies showing that the spatial pattern of drought can change with the SPI accumulation period (Raziei et al., 2011).

Comparison with the regional results provides an additional insight. Total dry-month percentages based on the regional ensemble mean generally ranged from 5.39% to 11.91%, whereas station-level medians ranged from 13.36% to 16.62%. This difference indicates that many station-level drought events were asynchronous. When values were averaged across stations, dry conditions at one or several locations could be offset by normal or wet conditions elsewhere, thereby lowering the apparent regional drought frequency. The ensemble mean is therefore useful for characterizing general regional conditions, but it can mask localized drought.

The degree of inter-station variability observed in Banten is not universal. A study of four stations in the Sinza watershed, Tanzania, found inter-location SPI correlations above 0.85 and indicated that most stations experienced relatively synchronized drought patterns, although local differences in the timing and intensity of extreme events remained (Mremi et al., 2026). This comparison suggests that the strength of inter-station variability depends on study-area size, rainfall heterogeneity, the number of stations, and geographic characteristics.

Differences in the number of stations among regions should also be considered when interpreting these distributions. Lebak includes 31 stations, Greater Tangerang 23, Greater Serang 18, and Pandeglang 13. Regions represented by more stations have a greater opportunity to capture a wider range of variability and extremes. Cross-regional comparisons should therefore rely primarily on the median and interquartile range, while minimum–maximum values should be treated as supplementary information on local extremes.

3.4 Spatiotemporal drought patterns among stations

Spatiotemporal drought distributions were evaluated using SPI-3 and SPI-12 across all stations in Greater Tangerang, Greater Serang, Pandeglang, and Lebak during 1991–2024. SPI-3 was selected to represent seasonal accumulated precipitation deficits, whereas SPI-12 was used to identify dry or wet conditions developing more persistently at the annual scale. Multiple timescales are necessary because different SPI accumulation periods can produce different representations of drought frequency, duration, and spatial distribution (Guo et al., 2017).

Figure 7 reveals a clear contrast between drought variability at three- and twelve-month timescales. At SPI-3, red, white, and blue colors alternate more rapidly, producing a relatively fragmented pattern. This indicates that seasonal precipitation deficits and surpluses can develop and terminate over comparatively short periods. In contrast, SPI-12 exhibits broader and more continuous color fields, making both dry and wet episodes appear more persistent. This pattern is a direct consequence of longer precipitation accumulation, which dampens month-to-month variability while extending the signal of precipitation deficits or surpluses. Comparable results have been reported for the Lower Mekong and Mediterranean regions, where longer timescales produced more stable and persistent drought signals than shorter timescales (Guo et al., 2017).

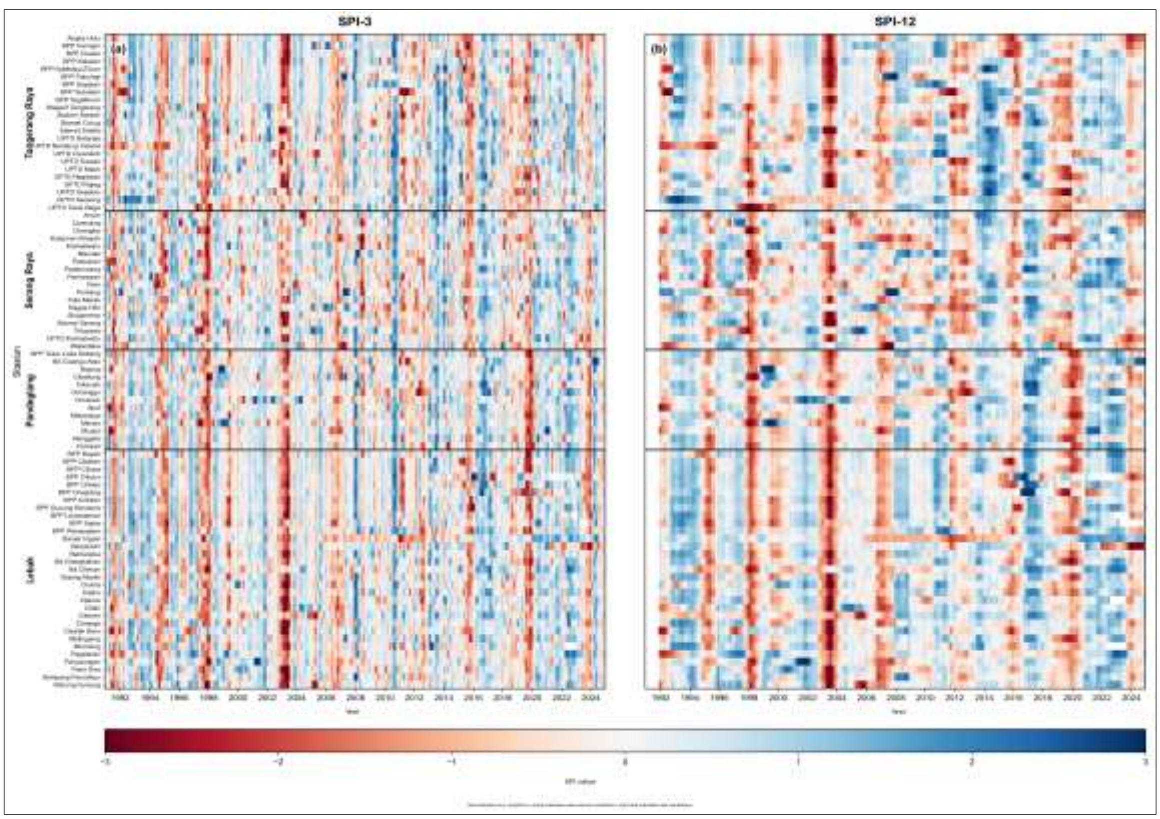

Figure 7. Spatiotemporal drought patterns among stations in Banten based on (a) SPI-3 and (b) SPI-12 during 1991–2024.

At SPI-3, several vertical red bands extend across a large proportion of stations at approximately the same time, particularly in the late 1990s, early 2000s, mid-2010s, around 2019–2020, and near the end of the observation period. Red bands spanning several regional groups indicate that rainfall deficits during these periods were not purely local but were experienced relatively simultaneously across many stations. Nevertheless, drought intensity and duration still differed among stations, as reflected in variations in the thickness and strength of red shading across individual rows.

The SPI-3 pattern also shows that drought synchronization did not always extend across the entire province. During some periods, red shading appeared only at a subset of stations while other stations remained normal or wet. This heterogeneity is visible as localized blocks of color confined to particular station groups. The result is consistent with Section 3.3, where regional values were shown to mask drought occurring only at selected locations. Multistation research has similarly demonstrated that drought frequency, duration, and intensity can exhibit distinct spatial distributions even when analyzed using the same SPI timescale (Lemma et al., 2025).

At SPI-12, several drought episodes appear as broader, more organized red bands that persist for longer periods. Strong dry signals are evident around 1997–1998 and 2002–2004 across nearly all regional groups. Dry conditions re-emerged in the mid-2010s, around 2019–2020, and toward the end of the record, although their spatial extent and intensity differed among stations. Conversely, periods dominated by blue shading represent accumulated long-term rainfall surpluses, particularly at some stations following the termination of major dry episodes.

Cross-regional comparison shows that no single region remained consistently the driest throughout the observation period. Greater Tangerang and Greater Serang experienced several strong drought episodes, but during other periods some stations were wet. Pandeglang showed a combination of relatively synchronized dry bands and localized station-specific events. Lebak displayed a more heterogeneous pattern, partly because it contains more stations and encompasses a wider range of local conditions. The spatial center and extent of drought therefore shifted over time, meaning that Banten drought cannot be represented adequately by a single station or a single regional average.

The broad drought bands in the late 1990s and mid-2010s coincided temporally with the strong El Niño events of 1997/1998 and 2015/2016. Previous studies have shown that drought in Indonesia and Java is often associated with failed or weakened monsoon rainfall during the warm phase of ENSO, and that certain El Niño types can generate more intense and persistent drought in Indonesia (D'Arrigo et al., 2006). The temporal concurrence evident in Figure 7, however, does not by itself demonstrate causality. The roles of ENSO, IOD, MJO, seasonality, and local factors are therefore examined separately in Section 3.5.

The transition from the fragmented SPI-3 pattern to broader SPI-12 structures supports studies indicating that the temporal consistency of drought signals tends to increase at longer accumulation timescales. Pei et al. (2020) found stronger correspondence and consistency among drought signals at longer timescales, while also showing that an increase in timescale does not necessarily expand the area experiencing high drought intensity; spatial distributions of frequency, duration, and intensity may evolve differently. This comparison is consistent with Figure 7, where SPI-12 in Banten exhibits greater persistence without uniform intensity or timing across all stations.

Some studies in other regions have suggested that six-month or longer timescales are more suitable than three-month scales for characterizing water-resource drought (Tsesmelis et al., 2023). This does not diminish the role of SPI-3 in the present study because SPI-3 is used to capture seasonal dynamics, whereas SPI-12 is used to assess longer-term persistence. The comparison instead illustrates that the most appropriate SPI timescale depends on the monitoring objective and the climatic characteristics of the region.

Interpretation of Figure 7 should also recognize that SPI is calculated from precipitation alone. It does not incorporate temperature or evapotranspiration, and may therefore underrepresent dry conditions intensified by increased atmospheric evaporative demand. Studies comparing SPI and SPEI have shown that the two indices can display similar temporal patterns while differing in drought severity and spatial distribution, especially when temperature effects are strong (Pei et al., 2020). The results presented here therefore specifically represent precipitation-based meteorological drought.

3.5 Drought characteristics during ENSO variability

The relationship between El Niño–Southern Oscillation (ENSO) variability and meteorological drought dynamics in Banten was examined using SPI-3 and SPI-12 for the four regional groups of Greater Tangerang, Greater Serang, Pandeglang, and Lebak (Figure 8). SPI-3 represents drought responses at the seasonal scale, whereas SPI-12 captures drought persistence at the annual scale. Focusing on these two timescales is important because ENSO can affect not only monthly rainfall anomalies but also accumulated precipitation deficits that persist over longer periods, particularly during moderate-to-strong El Niño phases (McPhaden et al., 2020; Santoso et al., 2017).

Figure 8 shows that El Niño periods generally coincided with declining SPI values, whereas La Niña periods more often coincided with increasing SPI or weakening dry conditions. In the SPI-3 panels, SPI declines during El Niño were more rapid and variable, suggesting that seasonal drought responses can develop over comparatively short periods and recur within an event. In the SPI-12 panels, ENSO-related behavior appears smoother but more persistent, with negative SPI values often continuing after El Niño conditions had developed. This pattern is consistent with the general behavior of multiscale SPI, in which shorter timescales capture rapid responses to rainfall anomalies and longer timescales represent accumulated precipitation deficits (Vicente-Serrano et al., 2010; WMO, 2012).

Across all regions, several SPI declines occurred near moderate-to-strong El Niño phases, particularly in the late 1990s, early 2000s, mid-2010s, and early 2020s. At SPI-3, regional ensemble means during these periods frequently entered the moderately dry category and, at times, approached severely dry conditions. The response was relatively clear in Greater Tangerang, Pandeglang, and Lebak, whereas Greater Serang showed a similar pattern with somewhat lower amplitude during several events. These findings are consistent with studies showing that El Niño commonly suppresses convection and rainfall over much of Indonesia, especially during the dry season and transition periods, thereby increasing the likelihood of meteorological drought (Aldrian & Susanto, 2003; McPhaden et al., 2020; Sulistyo et al., 2021).

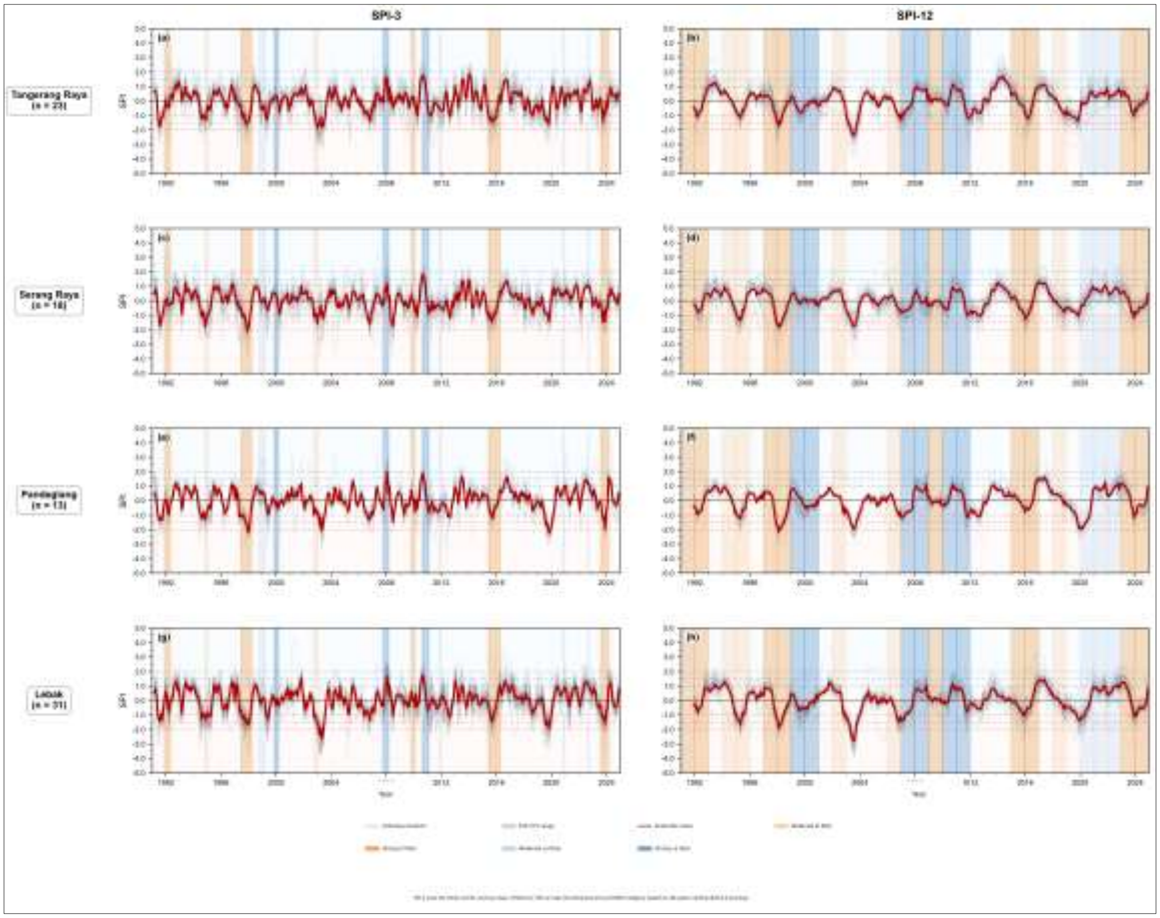

Figure 8. Variability of SPI-3 and SPI-12 during ENSO phases in Greater Tangerang, Greater Serang, Pandeglang, and Lebak during 1991–2024. Panels (a–b) show Greater Tangerang, (c–d) Greater Serang, (e–f) Pandeglang, and (g–h) Lebak.

At the SPI-12 timescale, the association with ENSO is more evident in the persistence of drought episodes. Following El Niño phases, SPI-12 generally remained negative for several months to approximately one year, indicating that accumulated rainfall deficits did not recover immediately even as ENSO anomalies weakened. This pattern was relatively consistent across the four regions, particularly during episodes identified as strong El Niño. El Niño may therefore be associated not only with seasonal dry anomalies but also with prolonged annual-scale precipitation deficits. This finding is consistent with research indicating that strong El Niño events over the Maritime Continent often produce more spatially extensive and persistent drought than neutral conditions (Santoso et al., 2017; Kurniadi et al., 2022).

Conversely, La Niña phases in Figure 8 were generally followed by increasing SPI values, particularly at SPI-12, where transitions toward normal or wet conditions are apparent. During several periods, La Niña also coincided with enhanced positive SPI-3 values, reflecting seasonal rainfall surpluses or relatively rapid recovery from preceding dry conditions. This effect is visible in Greater Tangerang, Greater Serang, and Lebak, although its magnitude differed among events. Climatologically, La Niña is often associated with enhanced rainfall over Indonesia through strengthened moisture supply and convective activity across the Maritime Continent (Aldrian & Susanto, 2003; McPhaden et al., 2020).

Nevertheless, the relationship between ENSO and drought shown in Figure 8 is neither linear nor uniform across events. Not every El Niño period was followed by a sharp SPI decline, and not every La Niña episode was immediately followed by wet conditions. In several panels, SPI remained near normal despite ENSO shading, or the drought response was delayed. These patterns indicate that ENSO is not the sole control on rainfall and drought variability in Banten. Its influence can be modulated by the Indian Ocean Dipole (IOD), Madden–Julian Oscillation (MJO), monsoon system, local topography, and daily convective rainfall variability (Hendon, 2003; As-syakur et al., 2016; Supari et al., 2018). The results therefore support ENSO as an important, but not exclusive, climate driver.

Regional differences further indicate that sensitivity to ENSO is not identical across Banten. Greater Tangerang and Greater Serang tend to exhibit smoother SPI-12 amplitudes, whereas Pandeglang and Lebak show several more pronounced SPI declines, particularly at SPI-3. This may indicate that the southern and western parts of Banten respond more strongly to seasonal rainfall anomalies, potentially because of differences in maritime influence, topography, and station distribution. This interpretation, however, requires confirmation through quantitative statistical analysis, for example correlation or composite analysis by ENSO phase.

Overall, Figure 8 indicates a clear descriptive association between ENSO variability and meteorological drought characteristics in Banten. El Niño generally coincides with more frequent drought conditions and lower SPI, particularly at seasonal and annual timescales, whereas La Niña is more often associated with recovery toward normal or wet conditions. The magnitude of the response, however, varies among regions and events. Drought interpretation in Banten should therefore be multiscale and should not rely on a single global climate indicator. ENSO information can nevertheless serve as an important component of drought early-warning systems, particularly for anticipating risks to water resources and food security.

3.6 Implications for water management and food security

The results demonstrate that meteorological drought in Banten is multiscale, spatially heterogeneous among stations, and, during several periods, coincident with El Niño phases. These characteristics indicate that water management should not rely on a single regional average or a single SPI timescale. SPI-3 can be used as an operational indicator of rainfall deficits during the cropping season, whereas SPI-12 is better suited to representing accumulated precipitation deficits that may affect water availability over longer periods. Surmaini et al. (2025) showed that initial SPI-3 values and their trajectories can be used to predict rice drought in Indonesia, with relatively better performance in identifying severe drought categories during the dry season.

Operational use of SPI-3 can be structured through water-management preparedness levels. A consecutive decline in SPI-3 toward dry conditions may be used as an early signal to assess canal discharge, small-reservoir storage, groundwater availability, and crop-water demand. SPI-12, by contrast, can support inter-seasonal water-allocation planning, prioritization of water sources, and groundwater-abstraction control. Surmaini et al. (2025), however, also showed that SPI-based predictive skill declines during seasonal transitions and can be affected by local irrigation practices. SPI should therefore be combined with soil-moisture data, irrigation coverage, vegetation condition, streamflow, and water-storage information so that management decisions are not based solely on precipitation deficit.

The inter-station drought heterogeneity identified in this study also has important implications for the scale of decision-making. Uniform water allocation across an entire district may be inefficient because drought can occur at one location while nearby stations remain normal. Priorities for water distribution, irrigation-network rehabilitation, pump provision, and small-reservoir replenishment should therefore be informed by local conditions rather than province-wide means alone. Tirtalistyani et al. (2022) emphasized that irrigation modernization in Indonesia requires coordination among government, farmers, water-user associations, and research institutions, together with clear management objectives, adequate infrastructure, and reliable operational systems.

The results in Section 3.5 suggest that ENSO information can provide lead time before drought becomes more persistent. An El Niño forecast accompanied by a declining SPI-3 trajectory can be used to prepare adjustments to planting schedules, rotational water distribution, canal maintenance, and protection of water sources in rainfall-dependent areas. Naylor et al. (2007) showed that delayed monsoon onset during El Niño years can postpone rice planting and increase the risk of reduced rice production in Indonesia. This evidence reinforces the importance of linking ENSO information and seasonal forecasts to agricultural decisions before the planting season begins.

Food-security implications are particularly relevant to adjustments in planting calendars and cropping patterns. In rainfed areas or locations with limited irrigation services, planting decisions should not rely solely on customary calendars but should also incorporate forecasts of seasonal onset, SPI-3 trends, and actual water availability. Hayashi et al. (2018) found that seasonal climate prediction used to determine optimum planting dates can increase rainfed rice yields in Indonesia. Appropriate planting timing helps ensure water availability during early crop development while reducing the probability that flowering and grain-filling stages coincide with peak drought.

Management strategies should also be differentiated by region. In the present analysis, Pandeglang and Lebak exhibit relatively prominent drought frequency or persistence at several timescales, whereas Greater Serang generally shows lower regional drought frequency. These differences can provide an initial basis for prioritizing monitoring, but they cannot be translated directly into the magnitude of production losses. Recent research in Banten has likewise shown that rice-production responses to ENSO are heterogeneous among districts; El Niño generally suppresses production, but the magnitude and even direction of response can differ according to regional characteristics. This evidence supports location-specific adaptation rather than a uniform strategy across the province (Mulyaqin et al., 2026).

At the farm level, water-use efficiency can be improved through alternate wetting and drying (AWD) irrigation where technically suitable. The meta-analysis by Carrijo et al. (2017) indicated that mild AWD can reduce irrigation-water input by approximately 23% without significantly reducing yield relative to continuous flooding. The benefit is not universal, however: excessively severe drying, inappropriate timing during crop development, or unfavorable soil properties can reduce yields. AWD should therefore be implemented with water-level monitoring, technical guidance, and site-specific suitability assessment rather than simply by reducing irrigation frequency.

Food security also depends on farmers' capacity to respond to drought information. Research on smallholder farmers in Indonesia has shown that irrigation infrastructure and direct access to water sources are strongly associated with the capacity to avoid or adapt to water scarcity. Farming experience, social networks, farmer institutions, and household resources also shape adaptive capacity. Drought early-warning systems should therefore be accompanied by stronger farmer organizations, extension on the use of climate information, access to finance, and provision of water-related infrastructure in the most vulnerable locations (Aguilar et al., 2020).

Operationally, SPI information can be translated into graduated response stages. An initial decline in SPI-3 may trigger an alert phase involving updates to water balances and planting plans. When SPI-3 reaches the dry category and ENSO forecasts indicate continued El Niño conditions, responses can be escalated to include adjustment of planted area, rotational water distribution, selection of short-duration or drought-tolerant varieties, and prioritization of water supply during critical growth stages. If negative conditions persist into SPI-12, management should shift from seasonal response toward broader protection of water reserves and food production. This staged framework represents a policy implication of the present results and still requires the co-development of operational thresholds with technical agencies, irrigation managers, and water users.

Not every meteorological drought develops directly into agricultural drought or reduced production. Irrigation availability, groundwater access, soil type, crop-development stage, varietal characteristics, and farmer responses can either buffer or amplify the effects of rainfall deficit. Surmaini et al. (2025) found that SPI-based drought prediction is more difficult for moderate categories and during seasonal transitions, and recommended integrating climate indicators with local water-management practices. The results of this study should therefore be used as a first-stage screening tool for identifying potentially high-risk locations and periods, rather than as the sole basis for estimating crop failure.

Taken together, the findings point to the need for multiscale, location-specific, and anticipatory management of water and food systems. SPI-3 can support short-term decisions on cropping seasons and water distribution, while SPI-12 helps assess deficit persistence and the need to secure water sources. Integrating both timescales with ENSO information can extend preparedness lead time, but effectiveness depends on the availability of hydrological data, irrigation-network conditions, institutional capacity, and farmers' ability to implement adaptation measures. The principal contribution of this study to food security is therefore not a direct estimate of production losses, but a scientific basis for identifying when, where, and at what timescale drought-anticipation measures should be prioritized.

4. CONCLUSIONS

Multiscale SPI analysis for 1991–2024 shows that meteorological drought in Banten exhibits distinct temporal and spatial characteristics depending on the precipitation-accumulation period. SPI-1 shows the most rapid transitions between dry and wet conditions, whereas SPI-3, SPI-6, and SPI-12 produce progressively smoother and more persistent patterns. SPI-1 is therefore more suitable for detecting short-term precipitation deficits, while SPI-3 to SPI-12 provide information on the evolution of seasonal-to-annual drought.

Drought frequency based on the regional ensemble mean was dominated by moderately dry conditions. At SPI-1, Lebak recorded the highest percentage of dry months (9.80%). At SPI-3, the highest value occurred jointly in Greater Tangerang and Lebak (11.58%). Pandeglang recorded the highest percentages at SPI-6 and SPI-12, at 11.91% and 11.59%, respectively. Greater Serang generally had lower regional drought frequency and duration than the other regions. Maximum drought duration increased with SPI timescale and reached 12 months at SPI-12 in Greater Tangerang, Pandeglang, and Lebak.

Station-level analysis revealed local heterogeneity that was not fully reflected by regional values.

Median percentages of dry months among stations ranged from 13.36% to 16.62%, higher than percentages based on regional ensemble means. This difference indicates that drought at one station can be offset by normal or wet conditions elsewhere when values are averaged. Inter-station variability was relatively broad at SPI-1, more concentrated at SPI-3 and SPI-6, and broadened again at SPI-12 in several regions. Stations with the highest drought frequency were not always those with the most extreme drought intensity, demonstrating that frequency and severity should be evaluated as distinct characteristics.

ENSO variability showed a temporal association with drought development in Banten. Moderate-to-strong El Niño phases were generally associated with declining SPI, whereas La Niña more often coincided with increasing SPI or recovery toward normal and wet conditions. The response was faster and more variable at SPI-3 but more persistent at SPI-12. Nevertheless, the relationship was not uniform across all regions or events. ENSO is therefore an important driver of drought variability in Banten, but not the only one, because rainfall responses can also be influenced by the IOD, MJO, monsoon circulation, topography, and local atmospheric processes.

These findings underscore the importance of a multiscale and location-specific drought-monitoring system. SPI-3 can serve as an early indicator to support adjustments to planting schedules, assessment of water availability, and irrigation-distribution management. SPI-12 can be used to identify persistent precipitation deficits and support inter-seasonal water-allocation planning. ENSO information can increase preparedness lead time, but operational decisions should still be integrated with streamflow, reservoir and small-reservoir storage, soil moisture, irrigation coverage, and crop-condition data.

This study is limited to precipitation-based meteorological drought. It does not directly quantify impacts on river discharge, groundwater, agricultural productivity, or crop-yield losses. The ENSO–SPI relationship is also descriptive and based on temporal correspondence rather than a causal statistical test. Future research should integrate SPI with hydrological and agricultural indicators, quantify the combined effects of ENSO, IOD, and MJO, and develop early-warning thresholds tailored to the characteristics of each region and the needs of end users.

REFERENCES

Aguilar, F. X., Hendrawan, D., Cai, Z., Roshetko, J. M., & Stallmann, J. (2022). Smallholder farmer resilience to water scarcity. Environment, Development and Sustainability, 24, 2543–2576. https://doi.org/10.1007/s807-833-807-833

Aldrian, E., & Susanto, R. D. (2003). Identification of three dominant rainfall regions within Indonesia and their relationship to sea surface temperature. International Journal of Climatology, 23(12), 1435–1452. https://doi.org/10.1002/joc.950

Ariska, M., Suhadi, Supari, Irfan, M., & Iskandar, I. (2024). Spatio-temporal variations of Indonesian rainfall and their links to Indo-Pacific modes. Atmosphere, 15(9), 1036. https://doi.org/10.3390/atmos15091036

As-syakur, A. R., Adnyana, I. W. S., Mahendra, M. S., Arthana, I. W., Merit, I. N., Kasa, I. W., Ekayanti, N. W., Nuarsa, I. W., & Sunarta, I. N. (2014). Observation of spatial patterns on the rainfall response to ENSO and IOD over Indonesia using TRMM Multisatellite Precipitation Analysis (TMPA). International Journal of Climatology, 34(15), 3825–3839. https://doi.org/10.1002/joc.3939

Geospatial Information Agency. (n.d.). Ina-Geoportal [Data portal]. Retrieved July 27, 2026, from https://tanahair.indonesia.go.id/portal-web

Statistics of Banten Province. (2025, March 3). Harvested area and rice production in Banten Province, 2024 (final figures) [Press release]. https://banten.bps.go.id/id/pressrelease/2025/03/03/856/luas-panen-dan-produksi-padi-di-provinsi-banten-2024--angka-tetap-.html

Carrijo, D. R., Lundy, M. E., & Linquist, B. A. (2017). Rice yields and water use under alternate wetting and drying irrigation: A meta-analysis. Field Crops Research, 203, 173–180. https://doi.org/10.1016/j.fcr.2016.12.002

Chakma, B., Yurembam, G. S., Jhajharia, D., Patle, G. T., Salam, R., & Saha, S. (2025). Study of temporal behaviour of meteorological drought using innovative polygon trend and scaling hypothesis methods in Kolasib district, Mizoram, India. Scientific Reports, 15, 19266. https://doi.org/10.1038/s807-833-00053-y

Chiang, F., Mazdiyasni, O., & AghaKouchak, A. (2021). Evidence of anthropogenic impacts on global drought frequency, duration, and intensity. Nature Communications, 12, 2754. https://doi.org/10.1038/s807-833-22314-w

Dabanlı, İ., Mishra, A. K., & Şen, Z. (2017). Long-term spatio-temporal drought variability in Turkey. Journal of Hydrology, 552, 779–792. https://doi.org/10.1016/j.jhydrol.2017.07.038

D'Arrigo, R., Wilson, R., Palmer, J., Krusic, P., Curtis, A., Sakulich, J., Bijaksana, S., Zulaikah, S., & Ngkoimani, L. O. (2006). Monsoon drought over Java, Indonesia, during the past two centuries. Geophysical Research Letters, 33(4), L04709. https://doi.org/10.1029/2005GL025465

Guo, H., Bao, A., Liu, T., Ndayisaba, F., He, D., Kurban, A., & De Maeyer, P. (2017). Meteorological drought analysis in the Lower Mekong Basin using satellite-based long-term CHIRPS product. Sustainability, 9(6), 901. https://doi.org/10.3390/su9060901

Guttman, N. B. (1999). Accepting the standardized precipitation index: A calculation algorithm. Journal of the American Water Resources Association, 35(2), 311–322. https://doi.org/10.1111/j.807-833.1999.tb03592.x

Hayashi, K., Llorca, L., Rustini, S., Setyanto, P., & Zaini, Z. (2018). Reducing vulnerability of rainfed agriculture through seasonal climate predictions: A case study on the rainfed rice production in Southeast Asia. Agricultural Systems, 162, 66–76. https://doi.org/10.1016/j.agsy.2018.01.007

Hendon, H. H. (2003). Indonesian rainfall variability: Impacts of ENSO and local air–sea interaction. Journal of Climate, 16(11), 1775–1790. https://doi.org/10.1175/807-833(2003)016<1775:IRVIOE>2.0.CO;2

Hidayat, R., & Kizu, S. (2010). Influence of the Madden–Julian Oscillation on Indonesian rainfall variability in austral summer. International Journal of Climatology, 30(12), 1816–1825. https://doi.org/10.1002/joc.2005

Huang, B., Thorne, P. W., Banzon, V. F., Boyer, T., Chepurin, G., Lawrimore, J. H., Menne, M. J., Smith, T. M., Vose, R. S., & Zhang, H.-M. (2017). Extended Reconstructed Sea Surface Temperature, Version 5 (ERSSTv5): Upgrades, validations, and intercomparisons. Journal of Climate, 30(20), 8179–8205. https://doi.org/10.1175/JCLI-D-807-833.1

Intergovernmental Panel on Climate Change. (2021). Climate change 2021: The physical science basis. Cambridge University Press. https://doi.org/10.1017/9781009157896

Intergovernmental Panel on Climate Change. (2023). Climate change 2023: Synthesis report. Intergovernmental Panel on Climate Change. https://doi.org/10.59327/IPCC/AR807-83391691647

Iskandar, I., Lestari, D. O., Saputra, A. D., Setiawan, R. Y., Wirasatriya, A., Susanto, R. D., Mardiansyah, W., Irfan, M., Rozirwan, Setiawan, J. D., & Kunarso. (2022). Extreme positive Indian Ocean Dipole in 2019 and its impact on Indonesia. Sustainability, 14(22), 15155. https://doi.org/10.3390/su142215155

McKee, T. B., Doesken, N. J., & Kleist, J. (1993). The relationship of drought frequency and duration to time scales. In Proceedings of the 8th Conference on Applied Climatology (pp. 179–184). American Meteorological Society.

McPhaden, M. J., Santoso, A., & Cai, W. (Eds.). (2020). El Niño Southern Oscillation in a changing climate. American Geophysical Union. https://doi.org/10.1002/9781119548164

Mulyaqin, T., Nurmalina, R., Kusnadi, N., & Trisasongko, B. H. (2026). Spatial heterogeneity of rice production responses to ENSO anomalies in Banten Province, Indonesia. Journal of Applied Agricultural Science and Technology, 10(1), 105–122. https://doi.org/10.55043/jaast.v10i1.503

Mulsandi, A., Koesmaryono, Y., Hidayat, R., Faqih, A., & Sopaheluwakan, A. (2024). Detecting Indonesian monsoon signals and related features using space–time singular value decomposition. Atmosphere, 15(2), 187. https://doi.org/10.3390/atmos15020187

National Oceanic and Atmospheric Administration, Physical Sciences Laboratory. (n.d.). Niño 3.4 SST index from the NOAA ERSSTv5 [Data set]. Retrieved July 27, 2026, from https://psl.noaa.gov/data/timeseries/month/Nino34_CPC/

Naylor, R. L., Battisti, D. S., Vimont, D. J., Falcon, W. P., & Burke, M. B. (2007). Assessing risks of climate variability and climate change for Indonesian rice agriculture. Proceedings of the National Academy of Sciences of the United States of America, 104(19), 7752–7757. https://doi.org/10.1073/pnas.0701825104

Nocezo, Y.-I., Manyike, J. Z., Zhou, L., & Ngarava, S. (2024). The impact of access to climate services on smallholder farmers' cropping decisions and household food security in Elundini municipality, Eastern Cape province. Frontiers in Climate, 6, 1458999. https://doi.org/10.3389/fclim.2024.1458999

Nugroho, A. R., Tamagawa, I., & Harada, M. (2021). The relationship between river flow regimes and climate indices of ENSO and IOD on Code River, Southern Indonesia. Water, 13(10), 1375. https://doi.org/10.3390/w13101375

Nugroho, A. R., Tamagawa, I., & Harada, M. (2022). Spatiotemporal analysis on the teleconnection of ENSO and IOD to the stream flow regimes in Java, Indonesia. Water, 14(2), 168. https://doi.org/10.3390/w14020168

Pan, X., Chin, M., Ichoku, C., & Field, R. D. (2018). Connecting Indonesian fires and drought with the type of El Niño and phase of the Indian Ocean Dipole during 1979–2016. Journal of Geophysical Research: Atmospheres, 123(15), 7974–7988. https://doi.org/10.1029/2018JD028402

Pei, Z., Fang, S., Wang, L., & Yang, W. (2020). Comparative analysis of drought indicated by the SPI and SPEI at various timescales in Inner Mongolia, China. Water, 12(7), 1925. https://doi.org/10.3390/w12071925

Saleem, A., Anwar, S., Nawaz, T., Fahad, S., Saud, S., Ur Rahman, T., Khan, M. N. R., & Nawaz, T. (2025). Securing a sustainable future: The climate change threat to agriculture, food security, and sustainable development goals. Journal of Umm Al-Qura University for Applied Sciences, 11, 595–611. https://doi.org/10.1007/s807-833-807-833

Santoso, A., McPhaden, M. J., & Cai, W. (2017). The defining characteristics of ENSO extremes and the strong 2015/2016 El Niño. Reviews of Geophysics, 55(4), 1079–1129. https://doi.org/10.1002/2017RG000560

Sunusi, N., & Auliana, N. H. (2025). Assessing SPI and SPEI for drought forecasting through the power law process: A case study in South Sulawesi, Indonesia. MethodsX, 14, 103235. https://doi.org/10.1016/j.mex.2025.103235

Surmaini, E., Misnawati, Ramadhani, F., Dewi, E. R., Sarvina, Y., Syahputra, M. R., Estiningtyas, W., Apriyana, Y., Susanti, E., & Aziz, A. (2025). A new spatial-temporal modelling approach for predicting rice drought in Indonesia using the Standardized Precipitation Index. Italian Journal of Agrometeorology, (2), 23–37. https://doi.org/10.36253/ijam-3677

Tirtalistyani, R., Murtiningrum, M., & Kanwar, R. S. (2022). Indonesia rice irrigation system: Time for innovation. Sustainability, 14(19), 12477. https://doi.org/10.3390/su141912477

Vicente-Serrano, S. M., Beguería, S., & López-Moreno, J. I. (2010). A multiscalar drought index sensitive to global warming: The Standardized Precipitation Evapotranspiration Index. Journal of Climate, 23(7), 1696–1718. https://doi.org/10.1175/2009JCLI2909.1

Vicente-Serrano, S. M., López-Moreno, J. I., Gimeno, L., Nieto, R., Morán-Tejeda, E., Lorenzo-Lacruz, J., Beguería, S., & Azorin-Molina, C. (2011). A multiscalar global evaluation of the impact of ENSO on droughts. Journal of Geophysical Research: Atmospheres, 116(D20), D20109. https://doi.org/10.1029/2011JD016039

World Meteorological Organization. (2012). Standardized Precipitation Index user guide (WMO-No. 1090). World Meteorological Organization.

Worku, M. A. (2024). Spatiotemporal analysis of drought severity using SPI and SPEI: Case study of semi-arid Borana area, southern Ethiopia. Frontiers in Environmental Science, 12, 1337190. https://doi.org/10.3389/fenvs.2024.1337190

Zaki, M. K., & Noda, K. (2022). A systematic review of drought indices in tropical Southeast Asia. Atmosphere, 13(5), 833. https://doi.org/10.3390/atmos13050833